LOCALIZATION OF LIGHT

Light in certain dielectric microstructures exhibits localized modes, similar to the localized wavefunctions of electrons in disordered solids. These microstructures show new effects in both classical optics and quantum electrodynamics.

Sajeev John

Since the beginning of scientific inquiry the nature of light has played a vital role in our understanding of the physical world. Physicists have marveled at the dual nature of light as both corpuscle and wave; we have harnessed the remarkable coherent properties of light through the use of lasers; and the quantum mechanics of the interaction of photons with matter continue to provide fascinating avenues of basic research. In essence, any alteration of electromagnetism, the fundamental interaction governing atomic, molecular and condensed matter physics, will lead to fundamentally new phenomena in all these areas.

At the microscopic level, ordinary matter exhibits behavior analogous to light waves. Electrons in a crystalline solid produce electrical conductivity by a constructive interference of various scattering trajectories. The wave nature of the electron gives rise to allowed energy bands and forbidden gaps for its motion in the solid. Disorder in the crystal hinders electrical conductivity, and for some energies the electronic wavefunctions are localized in space. This remarkable phenomenon, first discussed by Philip W. Anderson[1] in 1958 but fully appreciated only in the last decade, arises from wave interference, an effect common to both photons and electrons. Yet it is only recently that physicists have begun to ask whether scattering and interference can give rise to an analogous localization of light in an appropriate dielectric microstructure.[2] The semiconductor is an electronic material of fundamental importance in present day technology. Is there an analogous *photonic* material that may perform the same functions with light that semiconductors do with electrons? It is my aim in this article to describe such a new class of strongly scattering dielectric microstructures. Some of these microstructures will soon allow experimental confirmation of localization of light.

Light localization is an effect that arises entirely from coherent multiple scattering and interference. It may be understood purely from the point of view of classical electromagnetism. In traditional studies of electromagnetic wave propagation in dielectrics, scattering takes place on scales much longer than the wavelength of light. Localization of light, much the same as that of electrons, occurs when the scale of coherent multiple scattering is reduced to the wavelength itself. This is an entirely new and unexplored regime of optical transport with both fundamental and practical significance. Photons in a lossless dielectric medium provide an ideal realization of a single excitation in a static random medium at room temperature. (By contrast, studies of electrons in a disordered solid are hampered by the inevitable presence of electron–electron and electron–phonon interactions.) High-resolution optical techniques also offer the unique possibility of studying the angular, spatial and temporal dependence of wave intensities near a localization transition. On the practical side, multiple-scattering spectroscopy is already proving to be a valuable tool in studying the hydrodynamics of colloids, suspensions and other dense complex fluids. Multiply scattered electromagnetic waves already provide a valuable noninvasive probe in medicine.

Light localization, which occurs at the classical level, also has fundamental consequences at the quantum level. The quantum consequences are most readily seen in analogy with the electronic energy band gap of a semiconductor: Certain dielectric microstructures have no propagating modes in any direction for a range of frequencies and exhibit what is called a "complete photonic band gap." Such microstructures consist of periodic arrays of high-dielectric spheres or cylinders with diameters and lattice constants comparable to the wavelength of light. Figure 1 shows one such microstructure in which a complete bandgap for microwave radiation has been observed. Strictly speaking, such a structure has no allowed electromagnetic modes in the forbidden frequency range, although an impurity placed in the material will introduce localized modes in the gap, an effect that is also familiar in semiconductors. But in this photonic analog of a semiconductor, an impurity atom with a transition

Sajeev John is an associate professor of physics at the University of Toronto.

© 1991 American Institute of Physics

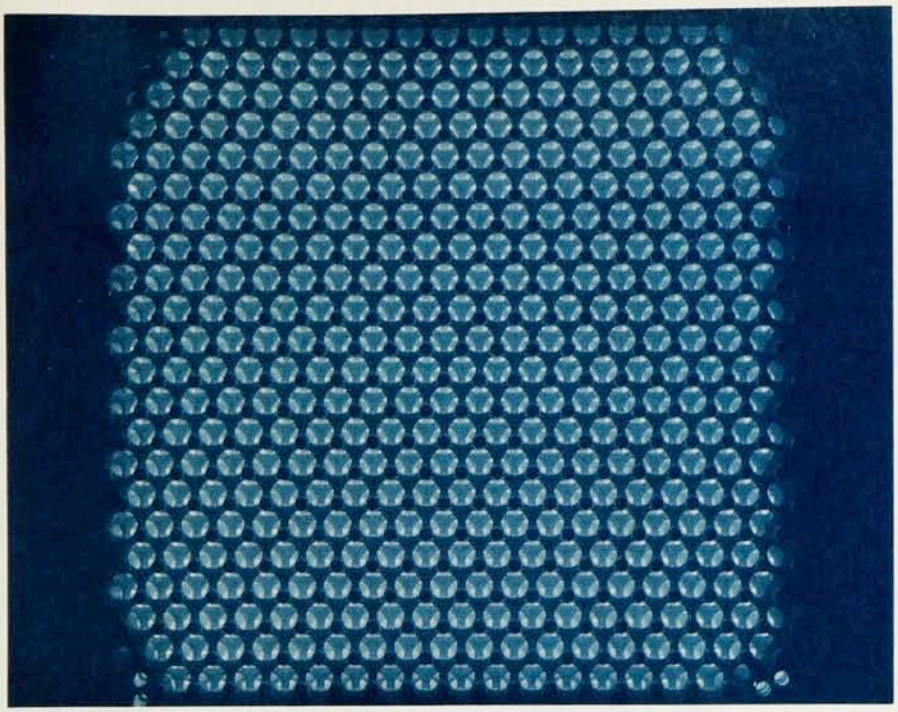

Dielectric structure that exhibits strong localization of electromagnetic waves. The patterned structure, which has the point-group symmetry of an fcc lattice, is made by drilling cylindrical holes in a material whose refractive index is 3.6. The pattern of holes is best understood by imagining an inverted cone with a 35.26° opening angle centered at each circle. The axes of the holes are three equally spaced radial lines on the surface of the cone. The crisscrossing of cylindrical air holes beneath the surface appears as small triangles inside the circles. The holes are 8 mm apart. Eli Yablonovitch and his colleagues at Bellcore have found that this sample exhibits a complete photonic bandgap for microwaves. **Figure 1**

frequency in the band gap will not exhibit spontaneous emission of light; instead, the emitted photon will form a bound state to the atom! Thus localization of light and the concomitant alteration of quantum electrodynamics suggest new frontiers of basic research spanning the disciplines of condensed matter physics and quantum optics.

Localized electrons and localized photons

Nature readily provides a variety of materials for the study of electron localization. In disordered solids localization is more often the rule than the exception. This is easily seen from the Schrödinger equation for an electron with effective mass m^* moving in a potential $V(\mathbf{x})$ that varies randomly in space:

$$\left[\frac{-\hbar^2}{2m^*}\nabla^2 + V(\mathbf{x})\right]\psi(\mathbf{x}) = E\psi(\mathbf{x}) \qquad (1)$$

Electrons with sufficiently negative energy E may get trapped in regions where the random potential $V(\mathbf{x})$ is very deep. The rate for electrons' tunneling out of the deep potentials depends on the probability of finding nearby potential fluctuations into which the trapped electron can tunnel. This rate increases as electron energy increases.

To quantify these ideas, consider $V(\mathbf{x})$ to have a root-mean-square amplitude V_{rms} and a length scale a on which random fluctuations in the potential take place. The correlation length a for the disorder defines an energy scale $\epsilon_a \equiv \hbar^2/(2m^*a^2)$. For example, in an amorphous semiconductor, a is the interatomic spacing, ϵ_a plays a role analogous to the conduction bandwidth of the semiconductor and the zero of energy corresponds to the conduction band edge of the corresponding crystal. In the weak disorder limit, $V_{\text{rms}} \ll \epsilon_a$, a transition takes place at an energy $E_c \simeq -V_{\text{rms}}{}^2/\epsilon_a$. Successive tunneling events allow an electron of energy greater than E_c to traverse the entire solid by a slow diffusive process and thereby conduct electricity, whereas electrons of energy lower than E_c are trapped and do not conduct electricity. Anderson first discussed this transition in 1958, and Nevill Mott called the critical value E_c the mobility edge.[3] For energies much greater than E_c, the scale on which scattering takes place grows larger than the electron's de Broglie wavelength and the electron traverses the solid with relative ease. However, if the disorder becomes stronger, so that $V_{\text{rms}} \gg \epsilon_a$, the mobility edge moves into the conduction band continuum ($E > 0$), and eventually the entire band may be filled with states exhibiting Anderson localization. Since disorder is a nearly universal feature of real materials, electron localization is likewise a ubiquitous ingredient in determining electrical, optical and other properties of condensed matter.

In the case of monochromatic electromagnetic waves of frequency ω propagating in an inhomogeneous but nondissipative dielectric medium, the classical wave equation for the electric field amplitude $\mathbf{E}$ may be written in a form resembling the Schrödinger equation:

$$-\nabla^2\mathbf{E} + \nabla(\nabla\cdot\mathbf{E}) - \frac{\omega^2}{c^2}\epsilon_{\text{fluct}}(\mathbf{x})\mathbf{E} = \epsilon_0\frac{\omega^2}{c^2}\mathbf{E} \qquad (2)$$

Here I have separated the total dielectric constant $\epsilon(\mathbf{x})$ into its average value ϵ_0 and a spatially fluctuating part $\epsilon_{\text{fluct}}(\mathbf{x})$. The latter plays a role analogous to the random potential $V(\mathbf{x})$ in the Schrödinger equation; it scatters the electromagnetic wave.

In a lossless material, in which the dielectric constant $\epsilon(\mathbf{x})$ is everywhere real and positive, several important observations based on the analogy between the Schrödinger (1) and Maxwell (2) equations are in order. First of all, the quantity $\epsilon_0\omega^2/c^2$, which plays a role analogous to an energy eigenvalue, is always positive, thereby precluding the possibility of elementary bound states of light in deep negative potential wells. It is also noteworthy that the laser frequency ω multiplies the scattering potential $\epsilon_{\text{fluct}}(\mathbf{x})$. Unlike an electronic system, where localization is enhanced by lowering the electron energy, lowering the photon energy instead leads to a complete disappearance of scattering. In the opposite high-frequency limit, geometric ray optics becomes valid and interference corrections to optical transport become less and less effective. In both limits the normal modes of the

electromagnetic field are extended, not localized. Finally, the condition that $\epsilon_0 + \epsilon_{fluct} > 0$ everywhere translates into the requirement that the energy eigenvalue be always greater than the effective potential $|(\omega^2/c^2)\epsilon_{fluct}(\mathbf{x})|$. Therefore, unlike the familiar picture of electronic localization, what we are really seeking when searching for localized light is an intermediate frequency window within the positive energy continuum that lies at an energy higher than the highest of the potential barriers! (See figure 2.) It is for this simple reason that ordinary dielectrics appearing in nature do not easily localize light.

Independent scatterers

The physics underlying the high- and low-frequency limits in the case of light can be made more precise by considering scattering from a single dielectric sphere. Consider a plane wave of wavelength λ impinging on a small dielectric sphere of radius $a \ll \lambda$ of dielectric constant ϵ_a embedded in a uniform background of dielectric constant ϵ_b in which the spatial dimension $d = 3$. The scattered intensity I_{scatt} at a distance R from the sphere can be a function only of the incident intensity I_0, the dielectric constants ϵ_a and ϵ_b and the lengths R, λ and a. In particular I_{scatt} must be proportional to the square of the dipole moment induced in the sphere, which scales as the square of the sphere volume, and by conservation of energy, it must fall off as R^{d-1} with distance from the scattering center:

$$I_{scatt} = f_1(\lambda, \epsilon_a, \epsilon_b)\frac{a^{2d}}{R^{d-1}} I_0 \qquad (3)$$

Since the ratio I_{scatt}/I_0 is dimensionless, it follows that $f_1(\lambda, \epsilon_a, \epsilon_b) = f_2(\epsilon_a, \epsilon_b)/\lambda^{d+1}$, where f_2 is another dimensionless function of the dielectric constants. The vanishing of the scattering cross section for long wavelengths as $\lambda^{-(d+1)}$, obtained here by purely dimensional arguments, is the familiar result explaining the blue of the sky.

The weak $\lambda^{-(d+1)}$ scattering is the primary reason that electromagnetic modes are extended in most naturally occurring three-dimensional systems. This behavior holds also for a dense random collection of scatterers. In that case, the elastic mean-free path l is proportional to λ^{d+1} for long wavelengths (see figure 3). This generalization of Rayleigh scattering to d spatial dimensions is also applicable to anisotropic dielectric scattering systems. For example, a layered random medium in which scattering is confined to directions perpendicular to the layers would be described by setting $d = 1$. Alternatively, a collection of randomly spaced uniaxial rods[4] in which scattering is confined to the plane perpendicular to the axes of the rods would be described by setting $d = 2$. A consequence of the scaling theory of localization, which applies to both electrons in disordered solids and electromagnetic waves in disordered dielectrics, is that all states are localized in one and two dimensions. For electromagnetic waves in disordered dielectrics the localization length ξ_{loc} diverges due to Rayleigh scattering in the low frequency limit, behaving as $\xi_{loc} \sim l$ in one dimension and $\xi_{loc} \sim l \exp(\omega l/c)$ in two dimensions.

It is likewise instructive to consider the opposite limit, one in which the wavelength of light is small compared to the scale of the scattering structures. It is well known that for scattering from a single sphere, the cross section saturates at a value of $2\pi a^2$ when $\lambda \ll a$. This is a result of geometric optics; the factor of two arises because of rays that are weakly diffracted out of the forward direction near the surface of the sphere. When discussing a dense random collection of scatterers, it is useful to introduce the notion of a correlation length a. On scales shorter than a, the dielectric constant does not vary appreciably except for the occasional interface where the physics of refraction and diffraction apply. The essential point is that the elastic mean-free path never becomes smaller than the correlation length. This classical elastic mean-free path l plays a central role in the physics of localization. Wave interference effects lead to large spatial fluctuations in the light intensity in the disordered medium. If $l \gg \lambda$, however, these fluctuations tend to average out to give a physical picture of essentially noninterfering, multiple scattering paths for electromagnetic transport. But when $l \to \lambda/2\pi$, interference between multiply scattered paths drastically modifies the average transport properties and a transition from extended to localized normal modes takes place. If one adopts the most naive version of the Ioffe–Regel[5]

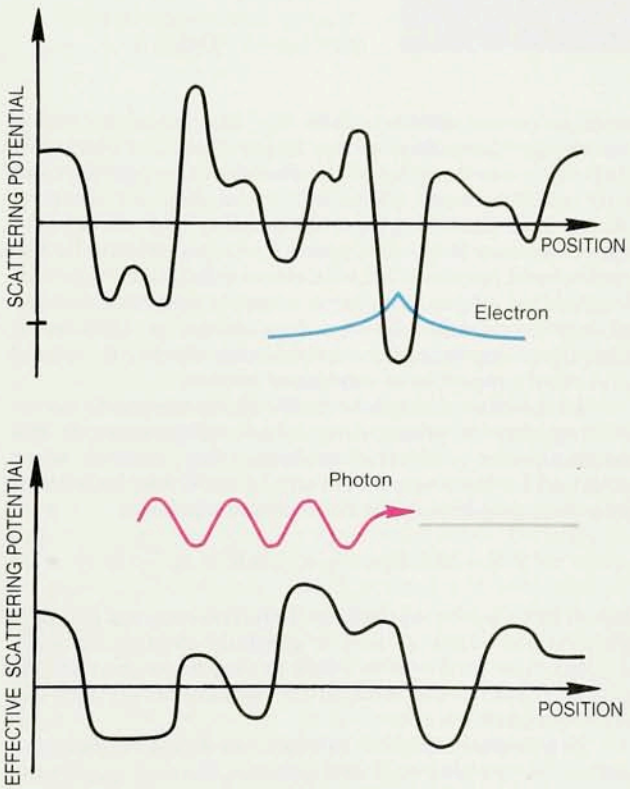

Scattering potential for electrons in a solid (black curve, top) and for photons in a random dielectric medium (black curve, bottom). The effective scattering potential for photons is $(\omega^2/c^2)\,\epsilon_{fluct}$, where ϵ_{fluct} is the spatially varying part of the dielectric. The electron (blue) can have a negative energy, and it can be trapped in deep potentials. By contrast, the eigenvalue $(\omega^2/c^2)\,\epsilon_0$ (gray line) of the photon (red) must be greater than the highest of the potential barriers if the dielectric constant $(\epsilon_0 + \epsilon_{fluct})$ is to be real and positive everywhere. **Figure 2**

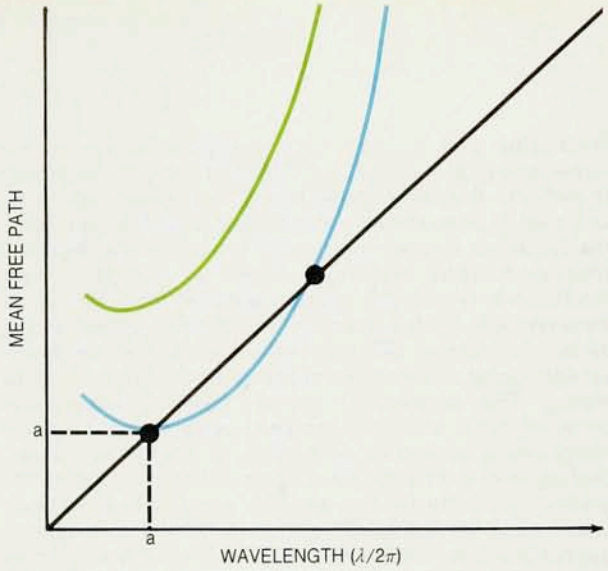

Condition for localization is that the classical transport mean free path l must approximately equal $\lambda/2\pi$ (black curve), where λ is the wavelength of light. In a medium with small variations in the index of refraction (green curve), the photon states are extended. In media with large variations in the refractive index (blue curve), weak scattering still dominates when $\lambda \ll 2\pi a$ or $\lambda \gg 2\pi a$, where a is the characteristic length scale of the medium. A window of localization opens at intermediate frequencies. **Figure 3**

condition, $2\pi l/\lambda \simeq 1$ for localization, with λ being the vacuum wavelength of light or the wavelength in an effective-medium theory for scattering, it follows that extended states are expected at both high and low frequencies. For strong scattering, however, there arises the distinct possibility, depicted in figure 3, of localization within a narrow frequency window when $\lambda/2\pi \simeq a$. It is this intermediate frequency regime that we wish to analyze in greater detail.

I will refer to the aforementioned criterion for localization as the free-photon Ioffe–Regel condition. The criterion is based on perturbation theory for multiple scattering of free photon states from point-like objects and on averaging over all possible positions of the scatterers. The latter assumes that all possible configurations of the scatterers are equally likely, or that the medium has an essentially flat structure factor on average.

A first correction to the above simple picture arises when one associates some nontrivial structure to the individual scatterers. For example, the scattering cross section can become quite large when the size of the scatterer is close to a multiple of λ, due to what are called Mie resonances in the scattering from dielectric spheres. These resonances have profound consequences for the elastic mean-free path. For spheres of dielectric constant ϵ_a and radius a embedded in a background of dielectric constant ϵ_b such that $\epsilon_a/\epsilon_b \simeq 4$, the first Mie resonance occurs at a frequency given by $\omega/c(2a) \simeq 1$ and yields a scattering cross section $\sigma \simeq 6\pi a^2$. For a relatively dilute collection of spheres of number density n, the classical elastic mean-free path is $l \sim 1/n\sigma = 2a/9f$, where f is the volume filling fraction of the spheres. Extrapolating this dilute scattering result to higher density, it should be apparent that for a filling fraction $f \simeq 1/9$, the free-photon Ioffe–Regel condition is satisfied on resonance. One might think that increasing the density of scatterers would further decrease the mean-free path and localize light. The existence of the resonance requires, however, that the "spheres of influence" of the scatterers do not overlap, whereas the fact that the cross section on resonance is six times the geometrical cross section indicates that a given sphere disturbs the wavefield over distances considerably larger than the actual sphere radius. Indeed, as the density increases beyond the value for the resonance, the spheres become optically connected and the mean-free path begins to increase rather than decrease. From the single-scattering or microscopic-resonance point of view, the free-photon criterion for localization is a very delicate one to achieve, a conclusion that Azriel Genack and Michael Drake[6] have shown in recent experiments on light scattering from randomly arranged dielectric spheres.

Coherent scatterers

The familiar example of Bragg scattering of an electron in a perfectly periodic crystal tells us that the approach

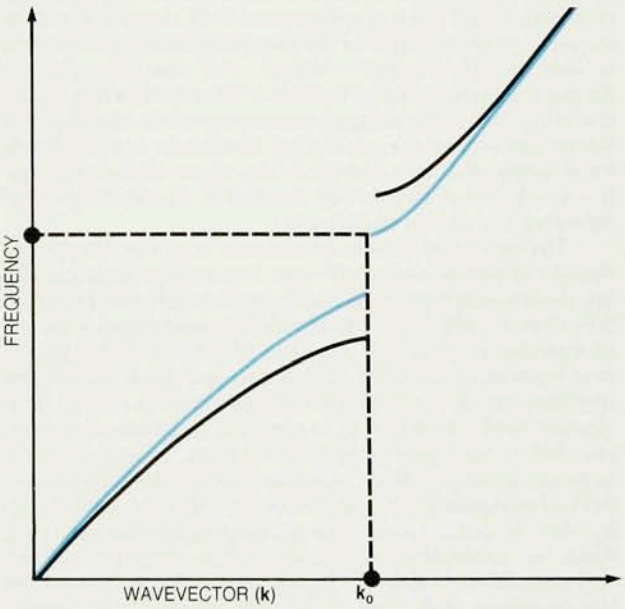

Dispersion relation for photons scattered coherently by a face-centered cubic lattice of dielectric spheres shows gaps for some values of **k**. The gap may persist over the entire Brillouin zone for a material composed of highly contrasting dielectrics. The two values of the gap shown (blue and black) stem from the two possible polarization states of the photon. **Figure 4**

based on independent, uncorrelated scatterers outlined above overlooks an important aspect of the problem. The example underlies what may be regarded as a fundamental theorem of solid state physics, namely, that certain geometrical arrangements of identical scatterers can give rise to large-scale or macroscopic resonances. The statistical average over all possible positions of the scatterers overlooks the consequences of this theorem. As we shall see, the theorem also has important consequences for light scattering in disordered systems in the limit of a high density of scatterers exhibiting short-range spatial order.

Consider a medium with dielectric constant whose

fluctuating part $\epsilon_{\text{fluct}}(\mathbf{x}) = \epsilon_1(\mathbf{x}) + V(\mathbf{x})$ is a sum of two terms, one $\epsilon_1(\mathbf{x}) = \epsilon_1 \Sigma_{\mathbf{G}} U_{\mathbf{G}} e^{i\mathbf{G}\cdot\mathbf{x}}$ that arises from a perfectly periodic Bravais superlattice of reciprocal vectors $\mathbf{G}$, and a small perturbation $V(\mathbf{x})$ arising from disorder. Here the dominant Fourier component $U_{\mathbf{G}}$ in the sum over the reciprocal lattice vectors is chosen so that the Bragg condition $\mathbf{k}\cdot\mathbf{G} = (1/2)\mathrm{G}$ may be satisfied for a photon of wavevector $\mathbf{k}$. Such a structure is attainable, albeit for low dielectric contrast between the scatterer and the background, using a suspension of charged polystyrene balls in water. The suspensions exhibit charge-induced face-centered cubic and body-centered cubic superlattice arrangements as well as a number of disordered phases. Setting $V(\mathbf{x}) = 0$ for the time being, the modulation of the photon spectrum by the periodic arrangement of scatterers may be estimated within a nearly free-photon approximation. Unlike electrons, which are described by a scalar wavefunction, the photon field has two polarization states and they are degenerate. If the electric field vector is perpendicular to the plane defined by the vectors $\mathbf{k}$ and $\mathbf{k} - \mathbf{G}$ (optical s wave), the resulting photon dispersion is the same as for scalar wave scattering. If, on the other hand, the polarization vector lies in the plane of Bragg scattering, the scattering amplitude is diminished by a factor of $\cos\theta$, where θ is the angle between $\mathbf{k}$ and $\mathbf{k} - \mathbf{G}$ (optical p wave). The associated photon dispersion relations are shown in figure 4.

The existence or near existence of a gap in the photon density of states is of paramount importance in determining the transport properties and localization of light.[2] The free-photon Ioffe–Regel condition discussed above assumes an essentially free-photon density of states and completely overlooks the possibility of this gap and the concomitant modification in the character of propagating states. The electric field amplitude of a propagating wave of energy just below the edge of the forbidden gap is to a good approximation a linear superposition of the free-photon field of wavevector $\mathbf{k}$ and its Bragg-reflected partner at $\mathbf{k} - \mathbf{G}$. As ω moves into the allowed band, this standing wave is modulated by an envelope function whose wavelength is given by $2\pi/q$, where q is the magnitude of the deviation of $\mathbf{k}$ from the Bragg plane. Under these circumstances the wavelength that must enter the localization criterion is that of the *envelope*. In the presence of even very weak disorder, the criterion $2\pi l/\lambda_{\text{envelope}} \sim 1$ is easily satisfied as the photon frequency approaches the band-edge frequency. In fact, near a band edge ω_c, $\lambda_{\text{envelope}} \sim |\omega - \omega_c|^{-1/2}$.

In the presence of a complete photonic band gap, the phase space (or allowed momentum values) available for photon propagation is restricted to a set of narrow, symmetry-related cones in the $\mathbf{k}$ space, analogous to the pockets of allowed electron states near a conduction band edge well known in semiconductor physics. Randomness in the positions of the dielectric scatterers leads to a mixing of all nearly degenerate photon branches, even when the disorder $V(\mathbf{x})$ is weak and treated perturbatively. In complete analogy with semiconductors, the band gap is replaced by a pseudogap consisting of localized states. (See figure 5.)

I have discussed in detail the two extreme limits: a structureless random medium for which the criterion $2\pi l/\lambda \simeq 1$ applies and a medium with nearly sharp Bragg peaks and a band gap for which $2\pi l/\lambda_{\text{envelope}} \simeq 1$ yields localization. Ivariably a continuous crossover occurs between these conditions as the structure factor of a high-dielectric material evolves from one limit to the other.

In the strong scattering regime required to produce a significant depression of the photon density of states, important corrections to the nearly free-photon picture of band structure emerge. Recent experimental studies[7] by Eli Yablonovitch on the propagation of microwaves in a dielectric material with refractive index 3.6 containing an fcc lattice of spherical air cavities show an almost complete photonic band gap when the solid volume fraction $f \simeq 0.15$. (See figure 1.) For a frequency range spanning about 6% of the gap center frequency, propagating electromagnetic modes are absent in all but a few directions. When the solid volume fraction is either increased or decreased from 0.15, the magnitude of the gap drops sharply. The existence of such an optimum value of sphere density illustrates a very fundamental principle concerning the origin of photonic band structures that is absent for electronic band structures. Bands of allowed electronic states arise in an ordinary semiconductor from coalescence of individual atomic orbitals. But there is no analog of the atomic orbital in the propagation of light through a periodic dielectric: A photon cannot be bound to a dielectric sphere. Instead, there are Mie scattering resonances, which occur when the diameter of the sphere is an integral multiple of the wavelength of light. A large photonic band gap arises when the density of dielectric spheres is chosen such that the Mie-resonances in the scattering by individual scatterers occur at the same wavelength as the macroscopic Bragg resonance of an array of the same scatterers. This principle may be

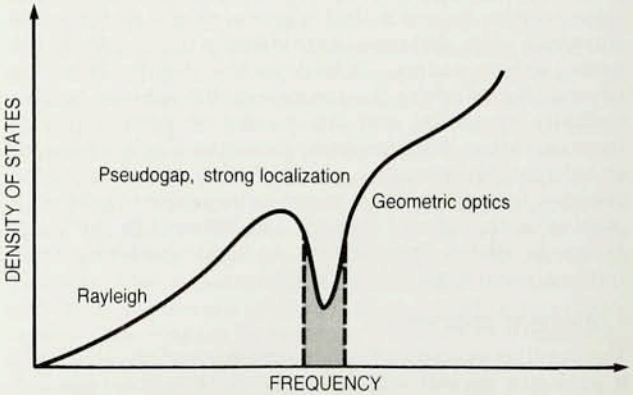

Density of states for photons in a disordered lattice of dielectric scatterers is dominated by Rayleigh scattering at low frequencies and by classical ray optics at high frequencies. The photonic gap of the perfect lattice of scatterers is now replaced by a pseudogap. The states in the pseudogap are strongly localized, in analogy with pseudogaps in amorphous semiconductors. The existence of a localization window (shaded region) is highly sensitive to the static structure factor of the dielectric material. **Figure 5**

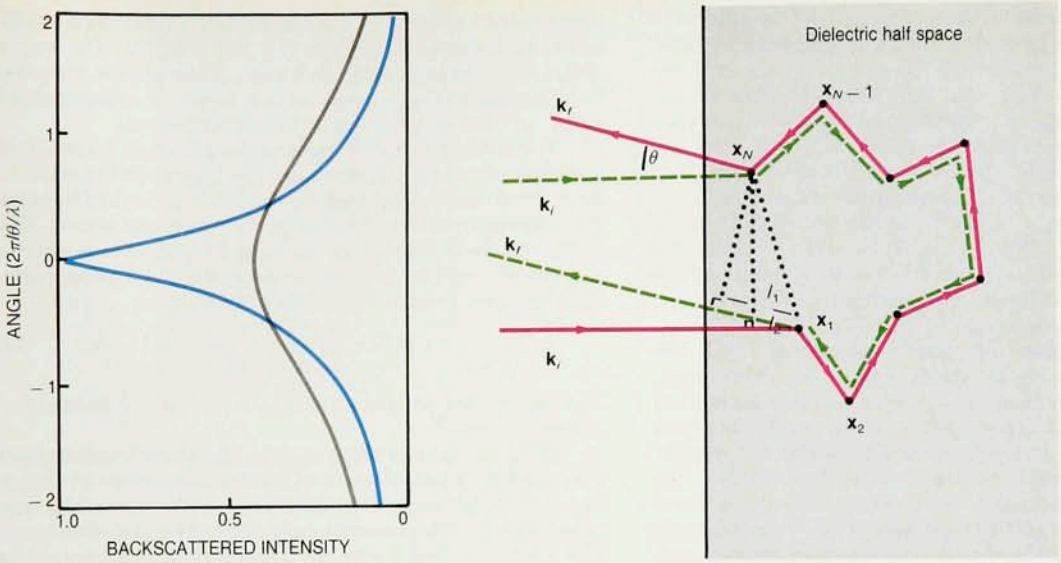

Coherent backscattering from a disordered dielectric, a precursor to localization, arises because a path (red) and its time-reversed partner (green) interfere coherently, giving rise to a backscattered intensity larger (at small angles between the incident and backscattered wave) than the diffuse reflected background one expects in the absence of interference (left panel). The origin of the intensity is set at the level of the background here. The intensity scale is in fractions of the background level. The higher of the two peaks shown (blue) describes backscattering in which the incident photon helicity is preserved; the smaller peak (gray) describes backscattered intensity when multiple scattering has flipped the helicity. **Figure 6**

illustrated by a simple example of one-dimensional wave propagation through a periodic array of square wells of width a and spacing L. Suppose the refractive index is n inside each well and is unity outside. Then the Bragg scattering condition is given by $\lambda = 2L$, where λ is the vacuum wavelength of light. The analog of a Mie-resonance in one dimension is a maximum in the reflection coefficient from a single well, and this occurs when a quarter wavelength fits into the well: $\lambda/(4n) = a$. Combining these two conditions yields the optimum volume-filling fraction $f \equiv a/L = 1/(2n)$. In analogy with the formation of an electronic band, the photonic band arises from the coalescence of Mie-scattering resonances of individual spheres.

Some very recent studies have suggested that the use of nonspherical scatterers or lattices with a nontrivial basis might be even more effective in producing a complete photonic band gap rather than a pseudogap.[8] Band structure calculations have shown that a complete gap may be produced with refractive index $n \gtrsim 2.0$ using a diamond lattice structure. Furthermore, Yablonovitch and his collaborators have found a complete microwave bandgap of width about 20% of the gap-center frequency using cylindrical rather than spherical dielectric microstructures.[8]

Coherent backscattering

The analogy between electrons and photons suggests the fabrication of a new class of dielectrics that are the photonic analogs of semiconductors. In one such class—the periodic array of dielectric scatterers—a photonic band gap arises. Positional disorder of these scatterers alters this picture. As in a semiconductor, the band gap is replaced by a pseudogap of localized states. In this section, I will describe the process by which a propagating photon becomes localized and discuss experimental manifestations of this phenomenon from the standpoint of classical electrodynamics.

A photon in a disordered dielectric propagates by means of a random-walk process in which the length of each random step is given by the classical transport mean-free path l. On length scales that are long compared to l, it is convenient to regard this as diffusion of light, with the diffusion coefficient given by $D = \frac{1}{3}cl$. Here c is some effective speed of light in the dielectric medium. Unlike a classical random walker, however, light is a wave, and this diffusion process must be described by an amplitude rather than a probability, so that interference between all possible classical diffusion paths must be considered in evaluating the transport of electromagnetic energy. In the case of optical waves propagating through a disordered dielectric medium, this interference effect has been vividly demonstrated by a beautiful series of experiments initiated by Y. Kuga and A. Ishimaru, by Meint P. van Albada and Ad Lagendijk and by Georg Maret and Pierre Etienne Wolf.[9] In these experiments, popularly known as observation of coherent backscattering, incident laser light of frequency ω enters a disordered dielectric half-space or slab and the angular dependence of the backscattered intensity is measured. For circularly polarized incident light, the intensity of the backscattered peak for the helicity preserving channel is a factor of two larger than the incoherent background intensity. Coherent backscattering into the reversed helicity channel, however, yields a considerably reduced backscattering intensity. The angular width of the peak in either case is roughly $\delta\theta \sim \lambda/(2\pi l)$.

Figure 6 shows a scattering process in which incident light with wavevector $\mathbf{k}_i = \mathbf{k}_0$ is scattered at points $\mathbf{x}_1, \mathbf{x}_2, \ldots \mathbf{x}_N$ into intermediate (virtual) states with wavevectors $\mathbf{k}_1, \mathbf{k}_2, \ldots \mathbf{k}_{N-1}$ and finally into the state $\mathbf{k}_N = \mathbf{k}_f$, which is detected. For scalar waves undergoing an identical set of wavevector transfers, the scattering amplitudes at the points $\mathbf{x}, \ldots \mathbf{x}_N$ are the same for the path (red) and the time-reversed path (dashed, green).

The nature of the interference between the two paths is determined entirely by their relative optical path lengths. The resulting relative phase is given by $\exp[i(\mathbf{k}_i + \mathbf{k}_f)\cdot(\mathbf{x}_N - \mathbf{x}_1)]$. In the exact backscattering direction $\mathbf{q} \equiv \mathbf{k}_i + \mathbf{k}_f = 0$, there is constructive interference and a consequent doubling of the intensity over the incoherent background. If the angle between $-\mathbf{k}_i$ and $\mathbf{k}_f$ is θ, then the coherence condition for small θ becomes $\mathbf{q}\cdot(\mathbf{x}_N - \mathbf{x}_1) = 2\pi\theta|\mathbf{x}_n - \mathbf{x}_1|\lambda < 1$. In the diffusion approximation $|\mathbf{x}_n - \mathbf{x}_1|^2 \simeq D(t_N - t_1) \simeq lL/3$, where D is the photon diffusion coefficient and L is the total length of the path. Thus paths of length L contribute to the coherent intensity for angles less than $\theta_m = \lambda/[2\pi(lL/3)^{1/2}]$.

At larger angles few paths contribute and the backscattered intensity decreases rapidly. E. Akkermans, Wolf and Roger Maynard have given a detailed derivation of the backscattered lineshape for scalar waves; Michael Stephen and Gabriele Cwilich have extended the derivation to electromagnetic waves.[10] Fred Mackintosh has shown that the discussion of lineshapes becomes most transparent in the helicity representation.[10] In addition to time-reversal invariance, there is the parity symmetry between the right- and left-handed circular polarization states. The symmetries may be broken by the Faraday effect and by natural optical activity, respectively. The calculated excess relative intensities with respect to the incoherent background, based on detailed calculations for the lineshapes, are also shown in figure 6. In the figure the intensity level is plotted relative to the diffuse background level: A level of 1.0 corresponds to a precise doubling of the light intensity in a particular direction relative to the background. The angle θ (measured in radians) is the angle that the wavevector of the backscattered light makes with respect to the vector $-\mathbf{k}_i$, where $\mathbf{k}_i$ is the incident direction.

The incorporation of coherent backscattering into the theory of diffusion of wave energy leads to a simple renormalization group picture of transport (see figure 7). When wave interference plays an important role in determining transport, as it does in coherent backscattering, the transport of wave energy is not diffusive in the simple sense that a photon performs a classical random walk. Fortunately, there is a way of applying the concept of classical diffusion even to this significantly more complicated situation, provided we make one major concession in our classical way of thinking: We must no longer think of the diffusion coefficient as a local quantity determined by a classical mean-free path and a speed of propagation; rather, we must consider the macroscopic coherence properties of the entire illuminated sample. In a random medium it is reasonable to expect that scatterers that are very far apart do not *on average* cause large interference corrections to the classical diffusion picture. (The word average here is very important. Changes in distant scatterers *can* give rise to significant fluctuations about the average.) Thus there exists a coherence length $\xi_{\text{coh}} \gtrsim l$ that represents a scale on which we must very carefully incorporate interference effects in order to determine the effective diffusion coefficient at any point within the coherence volume. As a specific example, consider a finite size sample of linear size L. By changing the scale of the sample, the number of diffusion paths that can interfere changes, giving rise to an effective diffusion coefficient $D(L)$ at any point within the sample that depends on the macroscopic scale L of the sample. In the vicinity of a mobility edge, on length scales L in the range $l < L < \xi_{\text{coh}}$, the transport of energy is subdiffusive in nature as a result of coherent backscattering, which gives a significant wave interference correction to classical diffusion. In this range, the spread of wave energy may be interpreted in terms of a scale-dependent diffusion coefficient that behaves roughly as $D(L) \simeq (cl/3)(l/L)$. On length scales that are long compared to ξ_{coh}, the photon resumes its diffusive motion except with a lower or renormalized value $(cl/3)(l/\xi_{\text{coh}})$ of the diffusion coefficient.

The scaling theory of electron localization, formulated by Elihu Abrahams, Anderson, Don Licciardello and T. V. Ramakrishnan[11] and based on the ideas of David Thouless, also summarizes the physical picture outlined above. The theory predicts that when the laser frequency ω is close to a mobility edge ω^*, the scale-dependent diffusion coefficient may be written in three dimensions as

$$D(L) \simeq \frac{cl}{3}\left(\frac{l}{\xi_{\text{coh}}} + \frac{l}{L}\right) \tag{4}$$

The theory also predicts that $\xi_{\text{coh}} \sim |\omega - \omega^*|^{-1}$ diverges as ω approaches ω^*.

The relevance of this result to an optical transmission experiment in the absence of dissipation or absorption is depicted in figure 7. Consider first the case in which the coherence length is short compared to the slab thickness. The time required for an incident photon to traverse the thickness L is given by $\tau(L) = L^2/D(L)$. For $l \lesssim \xi_{\text{coh}} \ll L$, the average displacement R of the photon as a function of time is that of classical diffusion $R \sim t^{1/2}$. In the case of incipient localization, described by $l \ll L \ll \xi_{\text{coh}}$, the diffusion coefficient has the value $D(L) = (cl/3)(l/L)$. The transit time from one face of the slab to the other now scales as $\tau(L) \sim L^3$. In other words a photon near the mobility edge suffers a "critical slowing down" and in time t traverses a distance $R \sim t^{1/3}$ rather than the longer distance $t^{1/2}$ traveled by a classical random walker.

Anomalies associated with incipient localization may appear in the total intensity transmitted through a slab of a disordered dielectric illuminated by a steady monochromatic plane-wave source. For the case of classical diffusion, the transmission coefficient T, defined as the ratio of the total transmitted intensity to the total incident intensity, is given by the relation $T = l/L$, where l is the classical elastic mean-free path. This may also be written as $T = 3D/cL$, from which one may infer a transmission coefficient $T \sim l^2/(\xi_{\text{coh}} L)$ for $l \lesssim \xi_{\text{coh}} \ll L$, but a new scale dependence $T \sim l^2/L^2$ appears in the incipient localization regime $l \ll L \ll \xi_{\text{coh}}$. Genack and Narciso Garcia have observed scale-dependent diffusion of precisely this nature in microwave scattering from a disordered collection of teflon and aluminum spheres (see cover).

In the case of electrons, a conservation law prevents their total number from changing. Photons, however, can be absorbed. The discussion of photon localization is therefore not complete without the analysis of wave propagation in a weakly dissipative disordered medium. By weak dissipation I mean that the inelastic mean-free path, or the typical distance between absorption events, is large compared to l but nevertheless smaller than the sample size L. This may be modeled by adding a small, constant imaginary part ϵ_2 to the dielectric constant, so that $\epsilon(\mathbf{x}) = \epsilon_0 + \epsilon_{\text{fluct}}(\mathbf{x}) + i\epsilon_2$. The optical absorption coefficient α is defined as the constant for the decay with distance of the intensity I_0 from a source: $I = I_0 e^{-\alpha x}$. The absorption coefficient describes the average absorption on scales long compared to the transport mean-free path l. It should not be confused with the scattering length of the incident beam, which may in fact be much shorter than l. Classical electromagnetic theory yields $\alpha = (\omega\epsilon_2/D)^{1/2}$ for radiation of frequency ω. The effects of coherent wave interference may be incorporated into this picture using the scaling theory of localization. For an infinite medium ($L = \infty$), the diffusion coefficient vanishes when the coherence length diverges. If $l_{\text{inel}} > \xi_{\text{coh}}$, it

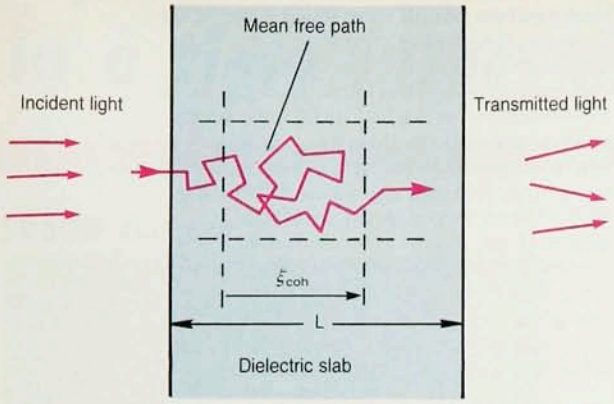

Optical transport near a photon mobility edge: For length scales L short compared to the coherence length ξ_{coh}, the transport of electromagnetic energy is subdiffusive due to coherent backscattering and must be described in terms of a length-dependent diffusion coefficient $D \simeq (c/3)(l/L)$. On scales longer than ξ_{coh}, the photon resumes its diffusive behavior *on average*, but the diffusion coefficient has the renormalized value $D \simeq (c/3)(l/\xi_{coh})$. **Figure 7**

follows that the increase in the absorption coefficient as the mobility edge frequency ω^* is approached from the extended-state side can be obtained from the change in the diffusion coefficient: Because $D(\omega) \sim |\omega - \omega^*|$, $\alpha(\omega)$ varies as $(\epsilon_2/|\omega - \omega^*|)^{1/2}$. On the other hand, if the coherence length exceeds the inelastic length, then l_{inel} acts as a long-distance cutoff for coherent wave interference. In this case, there is a residual diffusivity given by $D(\omega^*) \simeq (cl/3)(l/l_{inel})$. Since $l_{inel} = (D\tau_{inel})^{1/2}$ and $\tau_{inel} \sim 1/(\epsilon_2\omega)$, it follows that the residual diffusivity $D(\omega^*) \sim \epsilon_2^{1/3}$. Substituting the value of the residual diffusivity into the expression for α reveals that the absorption coefficient exhibits an anomalous scaling behavior with ϵ_2 $\alpha(\omega^*) \sim \epsilon_2^{1/3}$. The nontrivial critical exponent value of $\frac{1}{3}$ arises because of the critical slowing down of the photon as it approaches localization, which leads to a greater probability of absorption.

The anomalies in absorption associated with localization are a general indication of enhanced coupling of the electromagnetic field to matter. This leads to some profound new phenomena in atomic physics, which I will describe in the framework of quantum electrodynamics.

Quantum electrodynamics of localized light

When an impurity atom or molecule is placed in a dielectric exhibiting photon localization, the usual laws governing absorption and emission of light from the impurity must be reexamined. This is most easily seen in the strong localization limit, that is, in a dielectric exhibiting a complete photonic band gap. For a single excited atom with a transition energy to the ground state given by $\hbar\omega_0$ which lies within the band gap, there is no true spontaneous emission of light. The photon such an atom emits will find itself within the classically forbidden energy gap of the dielectric. If the nearest band edge occurs at frequency ω_c, this photon will tunnel a distance $\xi_{loc} \simeq c/(\omega_c|\omega_0 - \omega_c|)^{1/2}$ before being Bragg reflected back to the emitting atom. The result is a coupled eigenstate of the electronic degrees of freedom of the atom and the electromagnetic modes of the dielectric. (See figure 8.) This photon–atom bound state is the optical analog of an electron–impurity level bound state in the gap of a semiconductor.[13] The atomic polarizability, which is normally limited by the vacuum natural linewidth of the transition, can in the absence of spontaneous emission grow sufficiently large near resonance to produce a localized electromagnetic mode from the nearby propagating band states of the dielectric.

The fundamental weakness of the vacuum photon–atom interaction, as expressed by the fine structure constant $\alpha \equiv \frac{1}{137}$, is completely offset by this nearly unrestricted resonance. The alteration of the quantum electrodynamic vacuum by the dielectric host also appears in the spectroscopy of atomic levels. The ordinary Lamb shift of atomic levels is dominated by the emission and reabsorption of high-energy virtual photons. In a photonic band gap, this self dressing is dominated instead by the real, bound photon. In general, this will lead to some anomalous Lamb shift. If this level lies near a photonic band edge, a more striking effect is predicted to occur. In this case the atom is resonantly coupled to photons of vanishing group velocity. The resultant self-dressing of the atom is sufficiently strong to split the atomic level into a doublet. The atomic level is essentially repelled by its electromagnetic coupling to the photonic band edge. One member of the doublet is pulled into the gap and retains a photon bound state, whereas the other member is pushed into the continuum and exhibits resonance fluorescence. In the nearly free-photon approximation to electromagnetic band structure, the splitting of a hydrogenic $2p_{1/2}$ level is predicted to be as large as 10^{-6} $\hbar\omega_0$. This is analogous to the observed atomic level splittings, usually called Mollow splittings, which occur when an atom is subjected to an intense external laser field. For a dielectric exhibiting photon localization, the same effect may be achieved without any external field.

Further new phenomena are expected when a collection of impurity atoms is placed into the dielectric. A single excited atom can transfer its bound photon to a neighboring atom by a resonance dipole–dipole interaction. For a frequency ratio $\Delta\omega/\omega_0 = 0.05$ between the band gap and the band center, the photon tunneling distance ξ_{loc} is on the scale of $10a$, where the lattice constant a of the dielectric is itself on the scale of the photon wavelength. For impurity-atom spacings $R = 10$–1000 Å, the suppression of dipole–dipole interaction suggested by Gershon Kurizki and Genack can be neglected.[13] The matrix element M describing the hopping of a bound photon from one atom to another is given roughly by $M \sim \mu^2/R^3$, where the atomic dipole $\mu \simeq ea_0$ is given by the product of the electronic charge and the atomic Bohr radius a_0. This can be approximately related to the transition energy $\hbar\omega_0 \sim e^2/a_0$ by writing M as $(e^2/a_0)(a_0/R)^3$. When impurity atoms separated by $R \gtrsim 10$ Å have a finite density, it follows that photonic hopping conduction will occur through a narrow photonic impurity band of width $\sim(\hbar\omega_0)(a_0/R)^3$ within the larger band gap.

The occurrence of a photonic impurity band suggests new frontiers in nonlinear optics and laser physics. The strong coupling of light to matter may enhance nonlinear effects and cause them to be sensitive to the impurity–atom spacing. For example, when neighboring impurity atoms A and B are both excited, second harmonic generation may occur by the transfer of the bound state from atom A to atom B. Since atom B is already excited, the transferred photon creates a virtual state, and it may

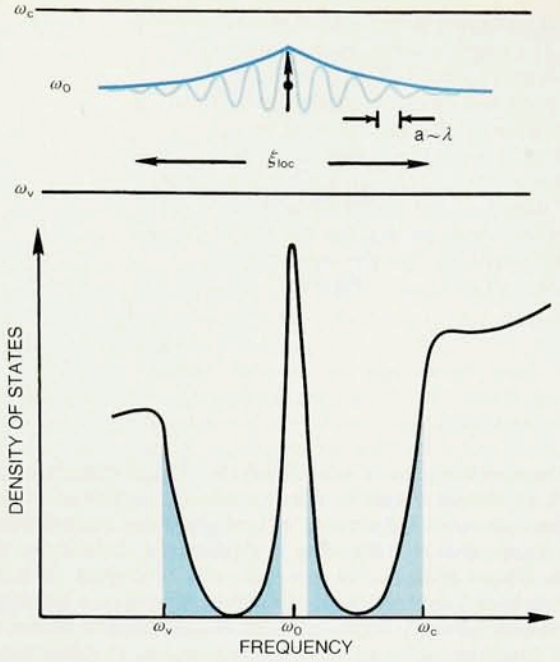

Photon–atom bound state (blue) is predicted when an impurity atom is placed in a dielectric such that the atom's transition frequency ω_0 lies in the localization gap $\Delta\omega$ of the dielectric. For $\Delta\omega/\omega_0 = 0.05$, the bound photon may tunnel a distance $\xi_{loc} \simeq 10a$, where a is the dielectric lattice spacing, before being Bragg reflected and reabsorbed by the atom. When several atoms are placed a distance $R \ll \xi_{loc}$ apart in the dielectric, the photons exhibit hopping conduction by means of the atomic resonance dipole–dipole interaction, which leads to the formation of a narrow photonic impurity band in the (larger) photonic band gap (bottom panel). **Figure 8**

then be emitted as a single photon of energy $2\hbar\omega_0$ outside of the photon band gap. The transfer can take place by dipole emission from atom A followed by a quadrupole Q virtual absorption by atom B. This process has an amplitude $\mu Q/R^4$. The resulting virtual excitation on atom B has odd parity, and it may then decay by a dipole emission process. The rate of spontaneous second harmonic generation is given by the square of the corresponding amplitude and depends sensitively, as $\omega_0\alpha^3(a_0/R)^8$, on the impurity–atom spacing.

Another significant question is that of laser activity within the impurity band when many photons are present. The impurity band defines a novel quantum many-body system in which the processes of spontaneous and stimulated emission of light are completely confined to and mediated by photonic hopping conduction between atoms. All photons are therefore more likely to contribute to the coherent, cooperative response of the many-body system. This must of course be balanced against non-electromagnetic relaxation events. For example, if the atom is embedded in the solid fraction of the dielectric, phonon-assisted emission of light as well as other homogeneous line-broadening effects will reduce the lifetime of a single photon–atom bound state. For an atom in the vacuum part of the dielectric, the dominant contribution to this lifetime is due to the finite absorption length l_{abs} of the orbiting photon. For a midgap atomic level the fraction of time that the system spends as an orbiting photon is about 10^{-7}. This corresponds to a lifetime on the scale of one minute for each kilometer of absorption length l_{abs}. The integrity of the photonic impurity band requires that all such homogeneous line-broadenings for a single atom be small compared to the overall frequency bandwidth of the impurity band. Inhomogeneous line broadening effects such as random strain fields in the solid will also affect the nature of electromagnetic transport within the photonic impurity band.

The implications of photon localization in quantum optics appear numerous and are only beginning to be explored. The fundamental challenge at present is one of materials science, namely the fabrication of three-dimensional arrays of lossless, high-refractive index scatterers of size comparable to the wavelength of light in which some degree of ordering can be induced. A possible solution to this fabrication challenge lies in the development of charged colloidal suspensions of high-index semiconductors, such as TiO_2. Even in the case of charged polystyrene spheres in water, which have a refractive index ratio of 1.5:1.3, significant changes in the rate of spontaneous emission from atoms placed in solution has been observed.[14] The charge-induced ordering of spheres leads to significant changes in the photon density of states even in this weak scattering case. Another possible solution to the materials problem is the refinement of etching techniques to drill cylindrical holes with diameters comparable to the wavelenth of visible light in bulk semiconductors. These possibilities suggest that the microwave experiments of Genack and his collaborators, demonstrating mobility edge behavior in a strongly disordered medium, as well as the result from Yablonovitch's group, demonstrating a complete microwave band gap in an ordered structure, may soon be extended to the optical wavelength regime. A clear demonstration of light localization and a complete elucidation of its consequences appear imminent.

References

1. P. W. Anderson, Phys. Rev. **109**, 1492 (1958).
2. S. John, Phys. Rev. Lett. **53**, 2169 (1984). S. John, Phys. Rev. Lett. **58**, 2486 (1987). P. W. Anderson, Phil. Mag. **B52**, 505 (1985).
3. N. F. Mott, *Metal-Insulator Transitions*, Taylor and Francis, London (1974).
4. I. Freund, M. Rosenbluh, R. Berkovits, M. Kaveh, Phys. Rev. Lett. **61**, 1214 (1989).
5. A. F. Ioffe, A. R. Regel, Prog. Semicond. **4**, 237 (1960).
6. A. Z. Genack, Phys. Rev. Lett. **58**, 2043 (1987). M. Drake, A. Z. Genack, Phys. Rev. Lett. **63**, 259 (1989).
7. E. Yablonovitch, Phys. Rev. Lett. **58**, 2059 (1987). E. Yablonovitch, T. J. Gmitter, Phys. Rev. Lett. **63**, 1950 (1989).
8. K. M. Ho, C. T. Chan, C. M. Soukoulis, Phys. Rev. Lett. **65**, 3152 (1990). K. M. Leung, Y. F. Lui, Phys. Rev. Lett. **65**, 2646 (1990). Z. Zhang, S. Satpathy, Phys. Rev. Lett. **65**, 2650 (1990). E. Yablonovitch, T. J. Gmitter, K. M. Leung (unpublished).
9. Y. Kuga, A. Ishimaru, J. Opt. Soc. Am. **A1**, 831 (1984). M. van Albada, A. Lagendijk, Phys. Rev. Lett. **55**, 2692 (1985). P. E. Wolf, G. Maret, Phys. Rev. Lett. **55**, 2696 (1985).
10. E. Akkermans, P. E. Wolf, R. Maynard, Phys. Rev. Lett. **56**, 1471 (1986). M. J. Stephen, G. Cwilich, Phys. Rev. **B39**, 7564 (1986). F. C. Mackintosh, S. John, Phys. Rev. **B37**, 1884 (1988).
11. E. Abrahams, P. W. Anderson, D. C. Licciardello, T. V. Ramakrishnan, Phys. Rev. Lett. **42**, 673 (1979).
12. A. Z. Genack, N. Garcia (unpublished).
13. S. John, J. Wang, Phys. Rev. Lett. **64**, 2418 (1990). G. Kurizki, A. Z. Genack, Phys. Rev. Lett. **61**, 2269 (1988).
14. J. Martorell, N. M. Lawandy, Phys. Rev. Lett. **65**, 1877 (1990).